

# Solar cycle dependence of polar cap patch activity

B. S. Dandekar

Air Force Research Laboratory, Space Vehicles Directorate, Hanscom AFB, Massachusetts, USA

Received 19 September 2000; revised 16 March 2001; accepted 25 October 2001; published 21 February 2002.

[1] Ionospheric  $f_oF_2$  data from two stations, Sondrestromfjord and Qaanaq, Greenland, for 4 years corresponding to four different levels of sunspot activity (sunspot number (SSN) =  $150 \pm 50$ ,  $125 \pm 50$ ,  $40 \pm 20$ , and  $10 \pm 10$ ) are used to study the dependence of occurrence and intensity of polar cap patches on solar cycle activity. At high sunspot activity, on the average, Sondrestromfjord sees six patches per day, and Qaanaq sees eight patches per day. At low sunspot activity the number drops to three per day at both stations. It is found that on a daily basis the polar cap patch activity is independent of the sunspot number for weaker patches ( $\geq 3$  MHz) but reduces with sunspot number for stronger patches ( $\geq 6$  MHz). Only at high sunspot activity, stronger patches are seen for 20% of the time. The duration of polar cap patches reduces from 50% at high sunspot activity (SSN = 150) to 15% at low sunspot activity (SSN = 10). It exhibits a seasonal dependence with a maximum in winter months. The diurnal maximum in polar cap patch activity at both stations occurs close to local magnetic noon. Assuming that polar cap patches are generated at high latitude (Sondrestromfjord) and drift to polar latitude (Qaanaq), only about 30% of patches seen at Qaanaq can be accounted for as originating at Sondrestromfjord. A reduction in patch activity with reduction in sunspot number is directly related to a reduction in the strength of the source: the tongue of ionization. The polar cap patches exhibit a weak dependence on the interplanetary magnetic activity index  $Kp$ . The distribution of the interplanetary magnetic field (IMF) for the patch occurrence very much resembles that of  $b_x$ ,  $b_y$ ,  $b_z$  of the IMF database. Over the solar cycle all these changes cover more than an order of magnitude of range. The effect of polar cap patch activity on communications operating at high-latitude regions is briefly discussed. **INDEX TERMS:** 2475 Ionosphere: Polar cap ionosphere; 2437 Ionosphere: Ionospheric dynamics; 2439 Ionosphere: Ionospheric irregularities; **KEYWORDS:** polar cap ionosphere, ionospheric dynamics, ionospheric irregularities, polar cap morphology

## 1. Introduction

[2] The polar cap patches produce strong radio scintillation, which can severely disrupt ground to satellite communication systems and could interfere strongly with the operation of space surveillance and navigation systems at high latitudes. Therefore it is essential to understand the morphology and long-term behavior of the polar cap patches as a phenomenon which affects space weather [Behnke *et al.*, 1995]. Most of the earlier information of polar cap patch activity came from case studies (see Buchau *et al.* [1983], Buchau and Reinisch [1991], and Dandekar and Bullett [1999] for references). Deployment of instruments at high and polar latitudes and satellite-based observations of polar cap patches improved our knowledge of polar cap patch morphology. For studying the morphology of polar cap

patches, Dandekar and Bullett [1999] used ionospheric  $f_oF_2$  measurements from the digital ionospheric sounding systems (DISS) [Reinisch *et al.*, 1983], ground-based radio scintillation measurements, and optical data from an all-sky imaging photometer for the period July 1989 to June 1990, at high solar activity (sunspot number (SSN) = 150). Their study used  $f_oF_2$  and scintillation measurements at 15-min intervals from ground stations at Sondrestromfjord, Greenland, and Qaanaq, Greenland. With the availability of  $f_oF_2$  data at Sondrestromfjord and Qaanaq covering a period of quite a few years, it is now possible to study long-term solar cycle dependence of polar cap patch activity. One reason for studying the long-term behavior of polar cap patches, with solar activity changing from averaged SSN equals 150 in 1989–1990 to averaged SSN equals 10 in 1996–1997, is to estimate the range of degradation of communication, surveillance, and navigation systems, which rely on the characteristics of the high-latitude and polar ionosphere.

This paper is not subject to U.S. copyright. Published in 2002 by the American Geophysical Union.

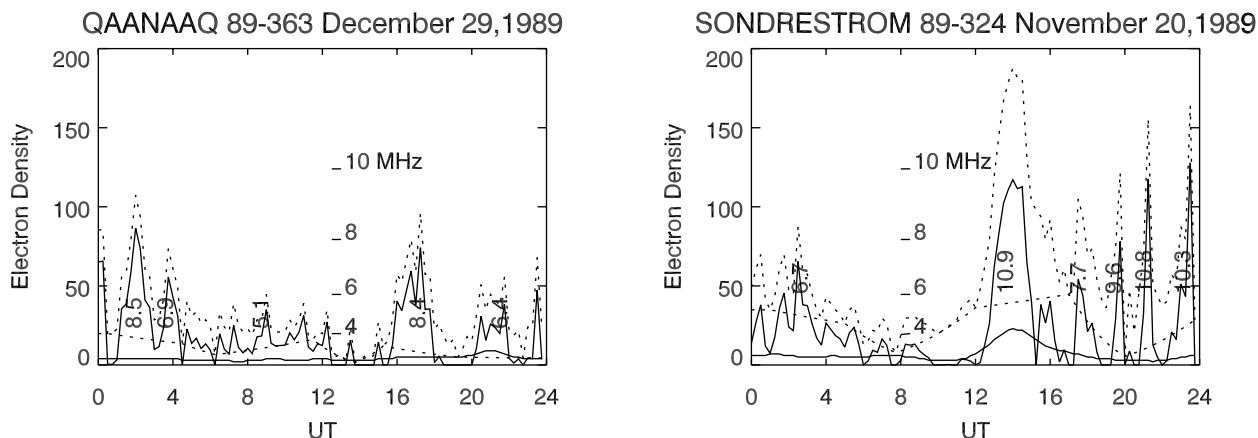


**Figure 1.** Appearance of polar cap patches at Qaanaaq and Sondrestromfjord, with respect to old and new baselines. The y scale for electron density extends from 0 to  $200 \times 10^4 \text{ cm}^{-3}$ .

[3] The solar cycle dependence of polar cap patch activity is presented in this paper. Observations of  $f_oF_2$  from DISS systems that were operated at Sondrestromfjord, Greenland, and Qaanaaq, Greenland, since 1989 are used. Data for 4 years are selected to represent different phases of solar cycle activity. Our definition of polar cap patch activity based on  $f_oF_2$  measurements has been improved. It is found that the overall polar cap patch activity follows general level variations of sunspot activity. The effects of polar cap patch behavior on communication systems will be briefly discussed.

## 2. Database

[4] Because the polar cap patch activity is known to be strongest in the winter period, for each phase of the solar cycle, annual  $f_oF_2$  data were selected from July (through December) to June. Four intervals were used: 1989–1990, 1991–1992, 1993–1994, and 1996–1997 with the annual averaged sunspot numbers (with standard deviation)  $150 \pm 50$ ,  $125 \pm 50$ ,  $40 \pm 20$ , and  $10 \pm 10$ , respectively, covering the period from the peak of solar cycle 22 to the minimum of solar activity at the beginning of solar cycle 23. The  $f_oF_2$  data from both the stations were usually collected at 15-min intervals. These data were gathered using DISS systems, and ionospheric parameters were extracted using the ARTIST-4 program developed by the University of Lowell, Lowell, Massachusetts. It seems possible that in the future the real-time data capability of these DISS systems can be gainfully employed for determining in situ disturbances by polar cap patch activity on communication systems. At Sondrestromfjord, Greenland (geographic latitude (GLat)

$67.0^\circ\text{N}$ , geographic longitude (GLong)  $50.6^\circ\text{W}$ , corrected geomagnetic latitude (CGMLat)  $75.16^\circ\text{N}$ , and CGM longitude (CGMLong)  $42.47^\circ\text{W}$ ),  $f_oF_2$  data were available for 266, 303, 355, and 297 days for the respective intervals. No  $f_oF_2$  data were available at Sondrestromfjord for May–June 1990; only 29% of the data were available for January 1990, and 26% of the data were available for June 1997. At Qaanaaq, Greenland (GLat  $77.5^\circ\text{N}$ , GLong  $68.7^\circ\text{W}$ , CGMLat  $86.71^\circ\text{N}$ , and CGMLong  $40.39^\circ\text{W}$ ),  $f_oF_2$  data were available for 341, 262, 297, and 364 days for the respective intervals. No  $f_oF_2$  data were available at Qaanaaq for the months September 1991, February 1992, and December 1993, and only 27% of the data were available for November 1993. In general, data availability at Qaanaaq, Greenland, was 84%, 55%, 62%, and 75% for the respective periods. The data availability at Sondrestromfjord, Greenland, was 39%, 53%, 64%, and 84% for the respective periods. The auxiliary data of planetary geomagnetic indices  $Kp$  used for the study were available from the National Geophysical Data Center (World Data Center, Boulder, Colorado). The National Space Science Data Center (Goddard Space Flight Center, Greenbelt, Maryland) provided the interplanetary magnetic field (IMF) data from the IMP 8 satellite. When the satellite was located inside the magnetosphere, the IMF data were not usable in this study. Thus only about 28% of the IMF data are useful for the study.

## 3. Analysis and Interpretation

[5] The difference between locations of the geographic and geomagnetic poles results in an asymmetric location of the auroral oval with respect to the geo-

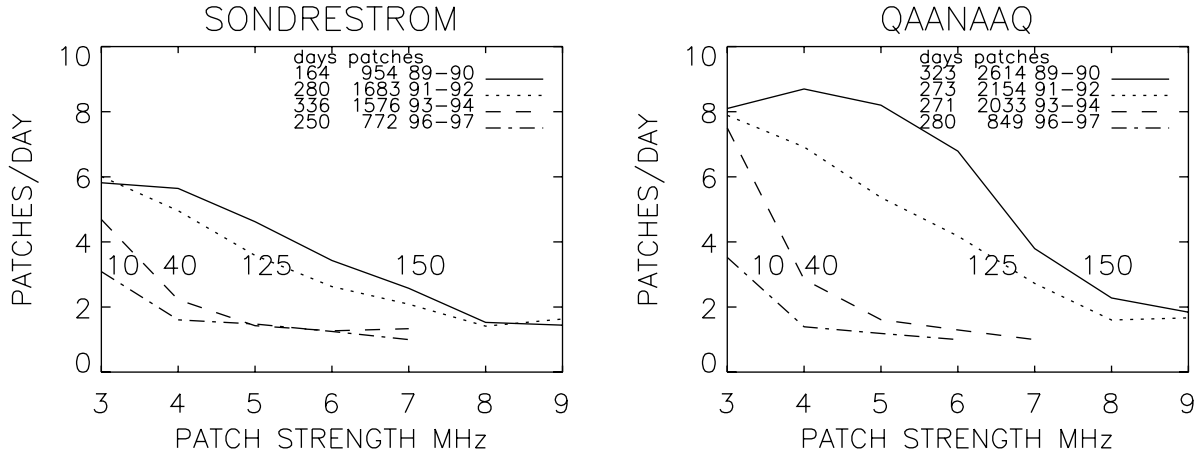


**Figure 2.** Averaged number of polar cap patches per day seen at Sondrestromfjord and at Qaanaaq at various levels of sunspot activity.

graphic pole. Thus Sondrestromfjord becomes an auroral station during daytime and a polar station at nighttime, whereas Qaanaaq is a polar station at all times. First an improved definition for identifying the polar cap patches from ionospheric observations will be presented. Then the diurnal, seasonal, and solar cycle behavior of the polar cap patch activity, and the extent of its effects on communication systems, will be considered. The dependence of the polar cap patch activity on planetary magnetic activity measured in terms of planetary geomagnetic activity index  $Kp$ , and on the interplanetary magnetic field (IMF), will be discussed.

### 3.1. Definition of DISS-Based Polar Cap Patches

[6] Using a variety of observations, optical data from an all-sky imaging photometer, radio scintillation measurements from ground-based receivers, and  $f_oF_2$  observations from DISS systems, *Dandekar and Bullett* [1999] showed that polar cap patches can be identified from  $f_oF_2$  data. They defined the strength (in megahertz) of the polar cap patch activity as the surplus of an electron density over an empirical baseline estimated at 2-hour intervals, from observed daily electron density ( $\propto f_oF_2^2$ ). To avoid having to use an occasional erratic daily baseline, a more stable and consistent monthly baseline of  $-1\sigma$  (standard deviation, refers to the sixteenth percent of the lowest population of the respective data set) level determined from the observations is used in this analysis. This change somewhat modifies the strengths shown in the previous report [*Dandekar and Bullett*, 1999] and alters the counts of the polar cap patches but does not change the overall pattern. The reason for selecting such a statistical baseline is that it can be extracted from

routine observations conducted by real-time operation of a system like the DISS sounder, which can be used for monitoring the polar cap patch activity.

[7] Figure 1 shows an example of polar cap patches determined using old and new baselines. The left-hand graph presents data from Qaanaaq on 29 December 1989, and the right-hand graph is for 20 November 1989 from Sondrestromfjord. In each graph a pair of dashed curves show observed electron density and a 2-hour interval empirical (old) baseline, whereas a pair of solid curves show the direct patch structures (new baseline is subtracted from the observed electron density) and the new ( $-1\sigma$  level) baseline mentioned above. The comparison of these two baselines shows that at some times they can vary significantly. The megahertz scale for measuring the polar cap patch strength (though the patch strength is in electron density, it is more convenient to refer to it in terms of megahertz, where 9 MHz is  $\sim 10^6$  el  $\text{cm}^{-3}$ ) is shown in each graph. The figure shows that the polar cap patch count and strengths referred to the respective baselines do not change significantly. A comparison with data from 1989–1990 for which both the old and new baselines were available showed that in the overall data set the polar cap patch count decreased by 15% at low patch strength (3 MHz) at both stations but did not change significantly at higher patch strengths.

### 3.2. Behavior of Polar Cap Patches With Respect to Solar Cycle Activity

[8] The number of polar cap patches exceeding a given strength was counted for each day. For each annual period an averaged number of polar cap patches per day was computed. Patches limited to a 15-min duration

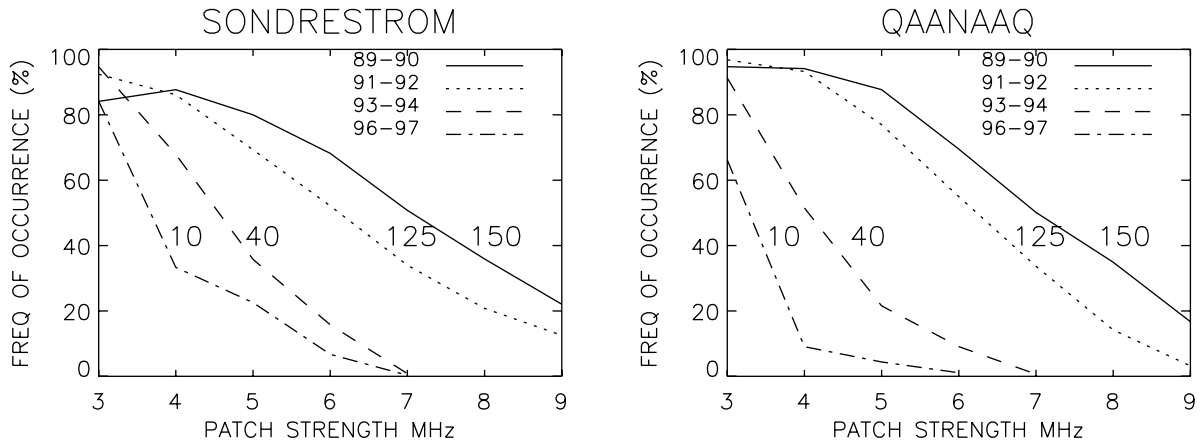


**Figure 3.** Occurrence of polar cap patches on a daily basis at Sondrestromfjord and Qaanaaq for various levels of sunspot activity.

(rate of data sampling/collection) were treated as noise in our data and were discarded from the analysis. The results are presented in Figure 2. The left-hand graph is for Sondrestromfjord, and the right-hand graph is for Qaanaaq. At the top center of each graph the total number days with polar cap patches and total number of polar cap patches with patch strength  $\geq 3$  MHz are listed for the respective periods. The curves are labeled with respective sunspot numbers. In general, Qaanaaq sees more polar cap patches than Sondrestromfjord. At Sondrestromfjord, on an average, six polar cap patches per day with strength  $\geq 3$  MHz are seen in the years 1989–1990 (SSN = 150) and 1991–1992 (SSN = 125). For these years the number drops to two patches per day for strength  $\geq 8$  MHz. At a patch strength  $\geq 3$  MHz the average number of polar cap patches per day reduced to

five and three for 1993–1994 (SSN = 40) and 1996–1997 (SSN = 10), and the highest patch strength for these years was 7 MHz. At Qaanaaq, eight polar cap patches are seen per day for a patch strength  $\geq 3$  MHz for all selected years, except 1996–1997 when the number is four polar cap patches per day. In general, more polar cap patches are seen at Qaanaaq than at Sondrestromfjord. One would expect to see relatively more patches at the polar station Qaanaaq than at the cusp region station Sondrestromfjord because the polar station would cover a wider region of the cusp than that covered by the individual station and because of breakup of patches drifting from the cusp region to polar latitudes. A similar behavior is seen at both the stations at corresponding levels of sunspot activity. With reduced sunspot activity there is a significant reduction both in patch strength and

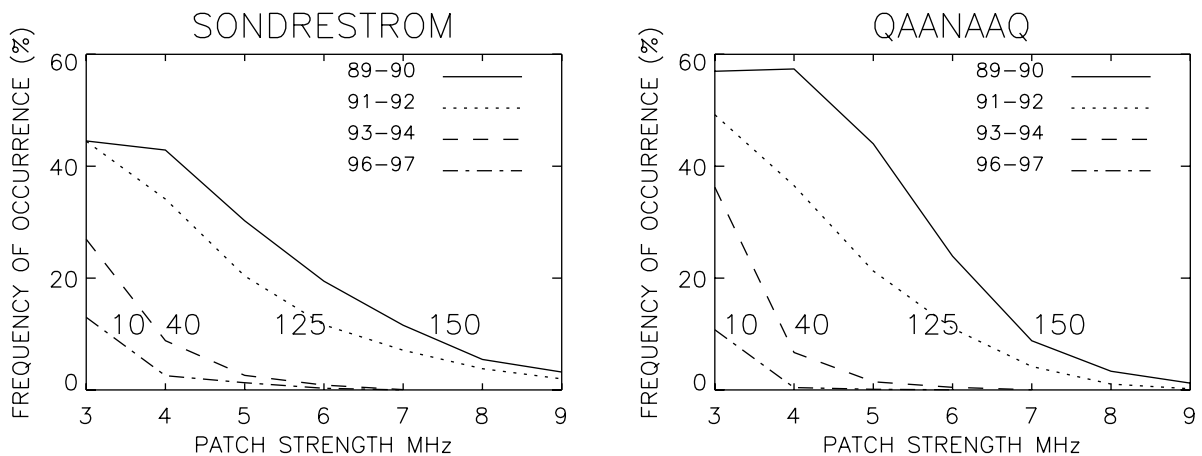


**Figure 4.** Occurrence of polar cap patches based on total period of observation at Sondrestromfjord and Qaanaaq for various levels of sunspot activity.

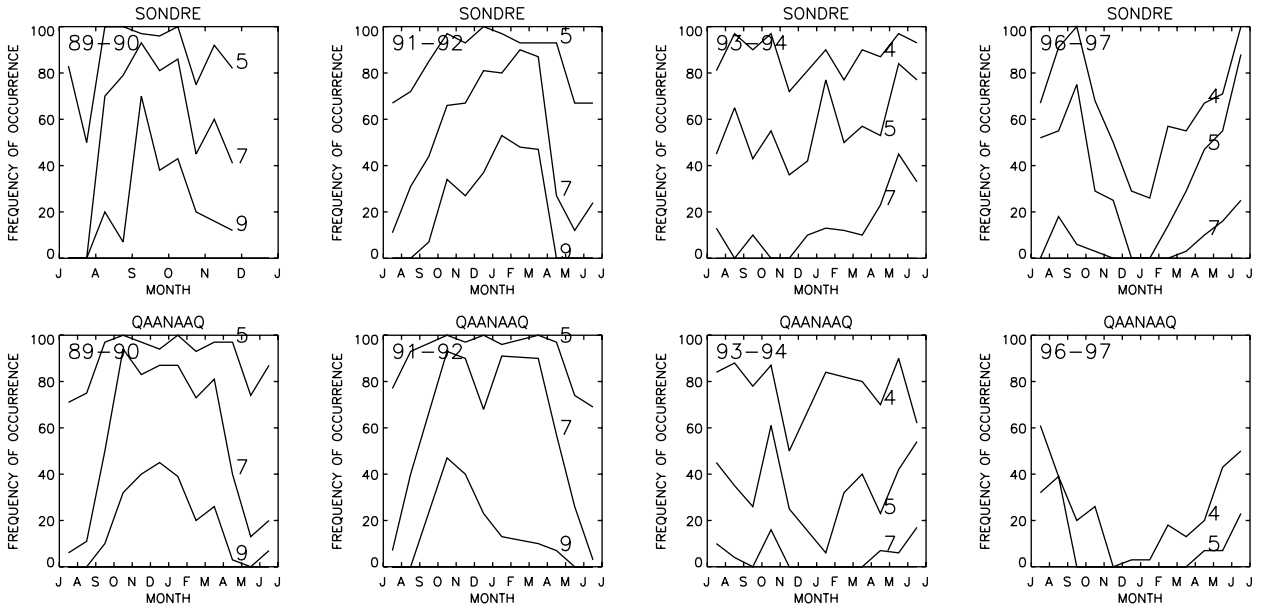
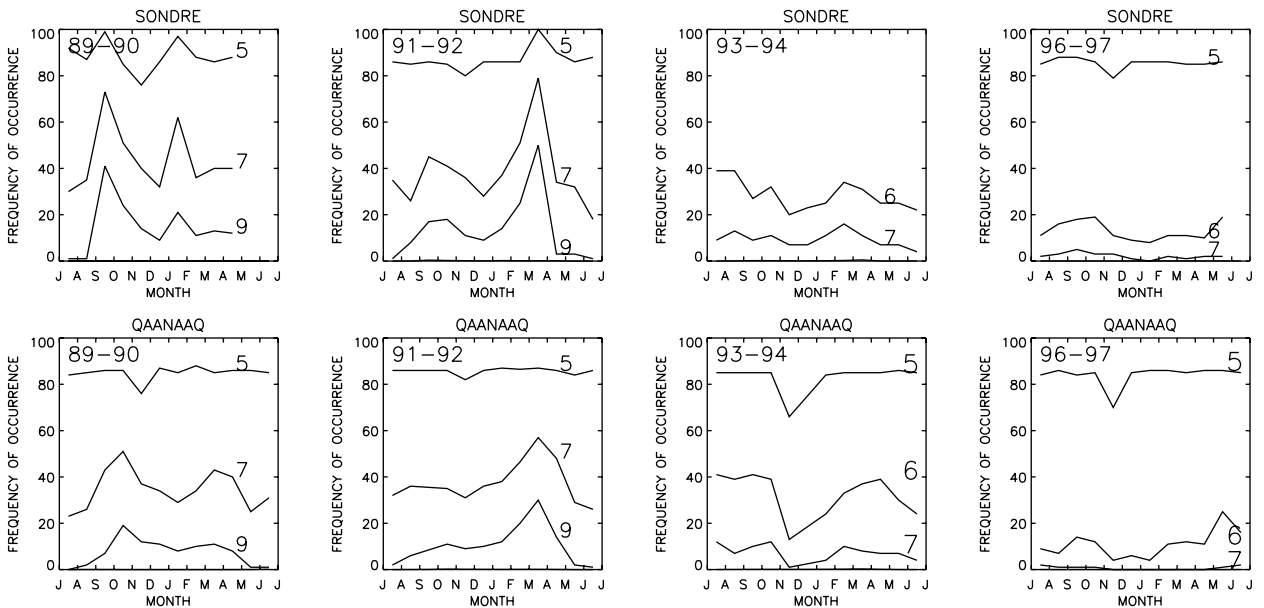


**Figure 5.** Seasonal behavior of polar cap patches at Sondrestromfjord and Qaanaaq with respect to daily occurrence.

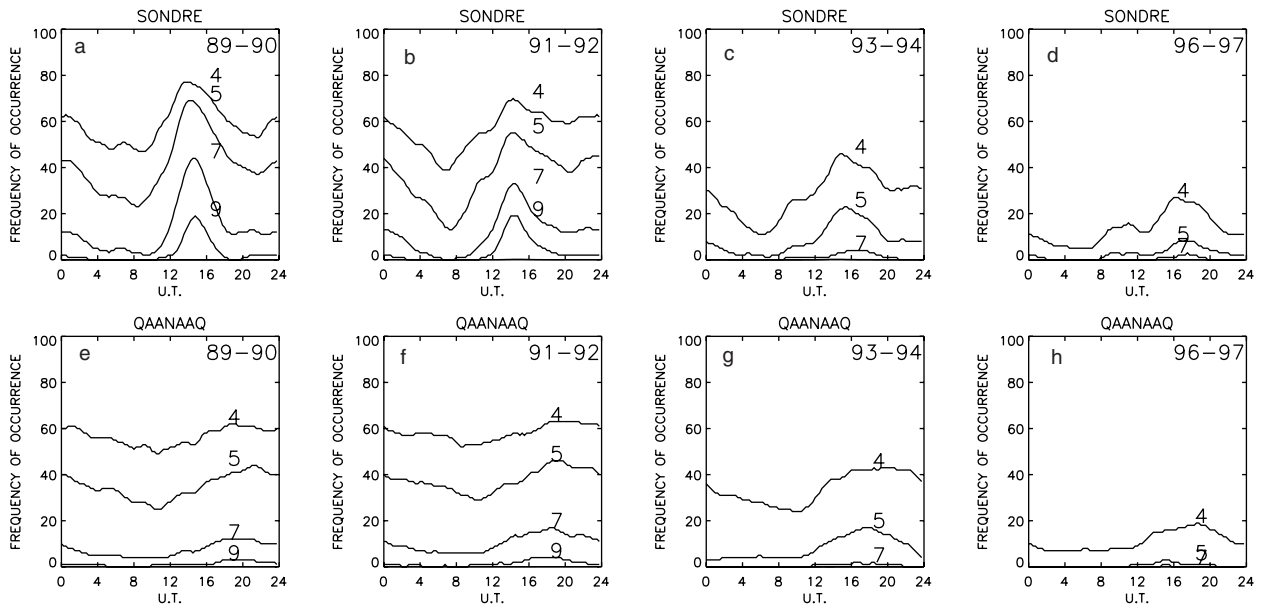
in number of polar cap patches seen per day. This similarity in the behavior at both stations indicates that these stations are observing the same phenomenon of polar cap patches. At Eureka (89° CGLAT), *McEwen and Harris* [1996] observed about six to eight patches per day in the winter months for 4 years (1990–1994). The

results of the present study are consistent with their observations, which are restricted to winter months and high to medium sunspot activity.

[9] The daily occurrence is checked for various minimum levels of patch strengths on the basis of a presence or absence of a polar cap patch for the whole data year.



**Figure 6.** Seasonal behavior of polar cap patches at Sondrestromfjord and Qaanaaq with respect to total observation time.



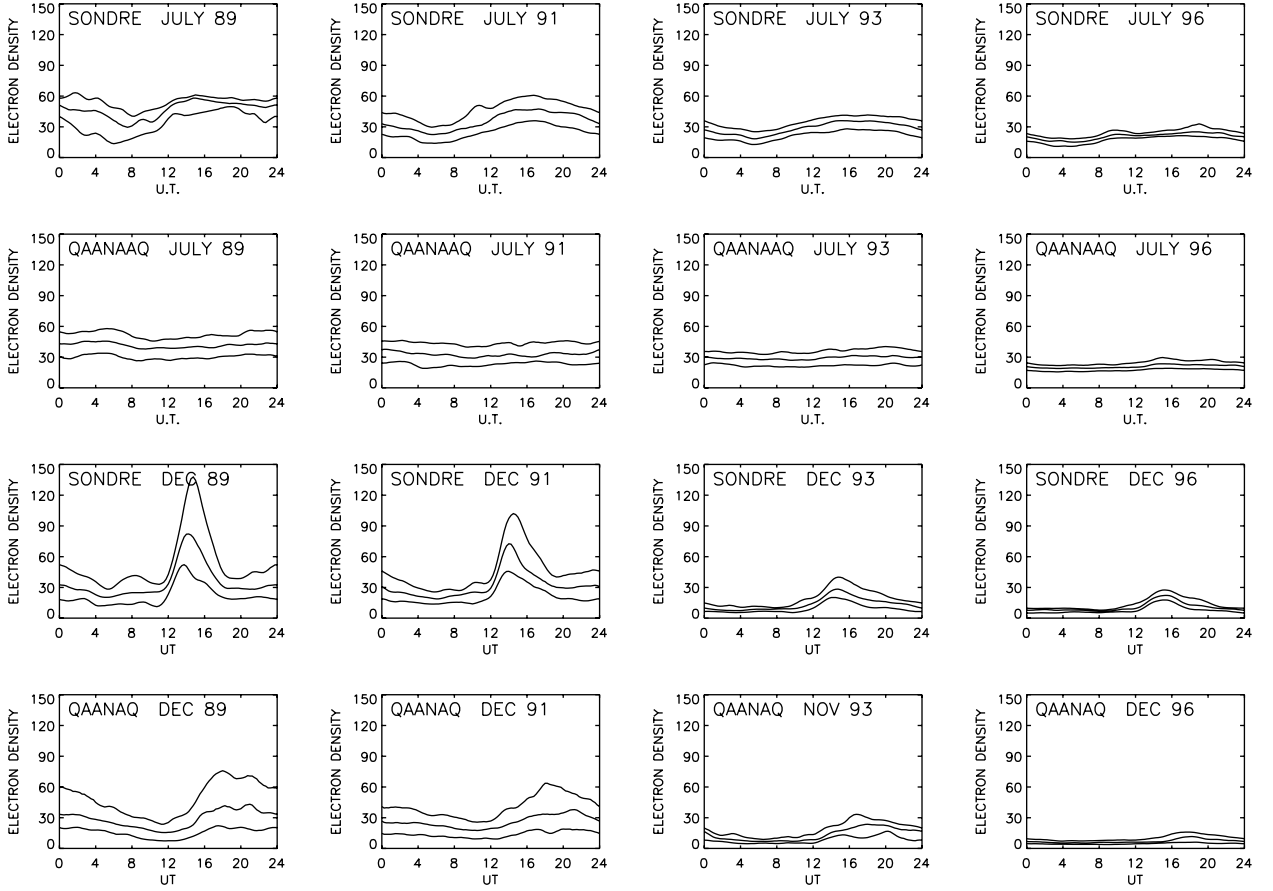
**Figure 7.** (a)–(h) Diurnal behavior of polar cap patch activity at Sondrestromfjord and Qaanaaq.

Figure 3 shows the polar cap patch occurrence on a daily basis. At lower patch strength  $\geq 3$  MHz, the polar cap patch occurrence is high,  $>80\%$ , and is independent of the level of sunspot activity. As the level of patch strength is increased, the daily occurrence reduces faster for reduced levels of sunspot activity. At low sunspot numbers of 40 and 10 no polar cap patches are seen with strengths  $\geq 7$  MHz, but polar cap patches are seen on 35% (and more) of the days at high sunspot activity. The behavior is very similar at both stations, supporting the assumption that both stations are observing the same polar cap patch phenomenon. The high-latitude station Sondrestromfjord mostly sees the tongue of ionization (TOI), which would be a source for generating polar cap patches, whereas the polar cap station Qaanaaq sees the polar cap patches. *Coley and Heelis* [1998b] used data from DE 2 (1981–1983) and DMSP F8 and F9 satellites (1988–1994) to study the polar cap patch behavior over the Northern and Southern Hemispheres. They did not find any significant difference in patch occurrence between high and moderate sunspot activity. Our results do show a good solar cycle dependence of the occurrence of polar cap patch activity.

[10] For each year all the time intervals with the data available were counted, along with the intervals for which the polar cap activity exceeded a given level of patch strength. Figure 4 shows the polar cap patch occurrence as a percent of the total time of observation. At high sunspot activity with minimum patch strength of

3 MHz, the polar cap patch occurrence is 45% at Sondrestromfjord during the high-sunspot-activity period of 1989–1992. It drops to 30% for 1993–1994 and to 15% at very low sunspot activity (SSN = 10) in 1996–1997. At Qaanaaq, which is closer to the geomagnetic pole, the polar cap patch activity is stronger than that at Sondrestromfjord. At both the stations, at high sunspot activity, for patch strength  $\geq 6$  MHz, the occurrence is 20%. At lowest sunspot activity the respective occurrences practically drop to 0%. Thus the patch occurrence reduced by a factor of 2 in patch strength (in electron content) and by a factor of 2 in duration of time with a change in sunspot activity. At Eureka, using meridian scanning photometers, for a 4-year period with a small sample (77 days), *McEwen and Harris* [1996] observed polar cap patch activity for 25% of the time. This compares well with our results.

[11] In Figures 2–4 the polar cap patch behavior at Qaanaaq and Sondrestromfjord displays tremendous similarity, suggesting that both stations are looking at the same patch structures. For determining a seasonal behavior of polar cap patch occurrence, daily presence or absence of the patch of a given minimum strength is checked on a monthly basis. The seasonal behavior of polar cap patches with respect to daily occurrence is shown in Figure 5. Graphs in each row are for the time periods selected to represent four levels of sunspot activity. In each graph the labels of the curves refer to levels exceeding the patch strengths. At high sunspot



**Figure 8.** Variation of electron density at Sondrestromfjord and Qaanaaq at median and  $\pm\sigma$  levels in summer and winter for various levels of sunspot activity. The y scale for electron density extends from 0 to  $200 \times 10^4 \text{ cm}^{-3}$ .

activity in 1989–1992, for patch strength  $\geq 5$  MHz the polar cap patch occurrence at both stations is high at  $>90\%$  from September to March, showing a weak seasonal dependence. At higher patch strengths the seasonal behavior peaks in winter months with occurrence as high as 40% for patch strength of 9 MHz. At medium to low sunspot activity there is no systematic seasonal dependence, but the level of occurrence reduces with declining sunspot activity. For example, at  $\geq 7$  MHz, for the winter months of October to March, it changes from 80% at high sunspot number to 20% at very low sunspot activity, showing a reduction of a factor of 4. In general, at low sunspot activity the polar cap patch occurrence is low compared to that at high sunspot activity, and an apparent minimum in winter months in seasonal behavior (that is, an apparent reversal in the seasonal behavior at low sunspot activity) is not understood.

[12] The seasonal behavior of polar cap patch occurrence is determined by checking the number of intervals

for which data are available against the total interval in which a patch exceeding a given strength is seen on a monthly basis. The seasonal behavior of polar cap patches with respect to the total period of patch activity is presented in Figure 6 with the same format as that of Figure 5. Basically, it reinforces the results found from Figure 5 and shows that there are two maxima in the seasonal behavior, one around October and another around February. *Basu et al.* [1995], *Coley and Heelis* [1995], and many others see the highest patch activity in winter months. *Sojka et al.* [1994] used a time-dependent ionospheric model (TDIM) to determine the seasonal dependence of the polar cap patches. Their model predicts general broad features like the winter maximum and peak occurrence between 2000 and 2400 UT but is unable to explain a dip in December–January seen in the observations.

[13] For each year the diurnal dependence of polar cap patch occurrence is determined by checking for the presence or absence of a patch exceeding a given strength

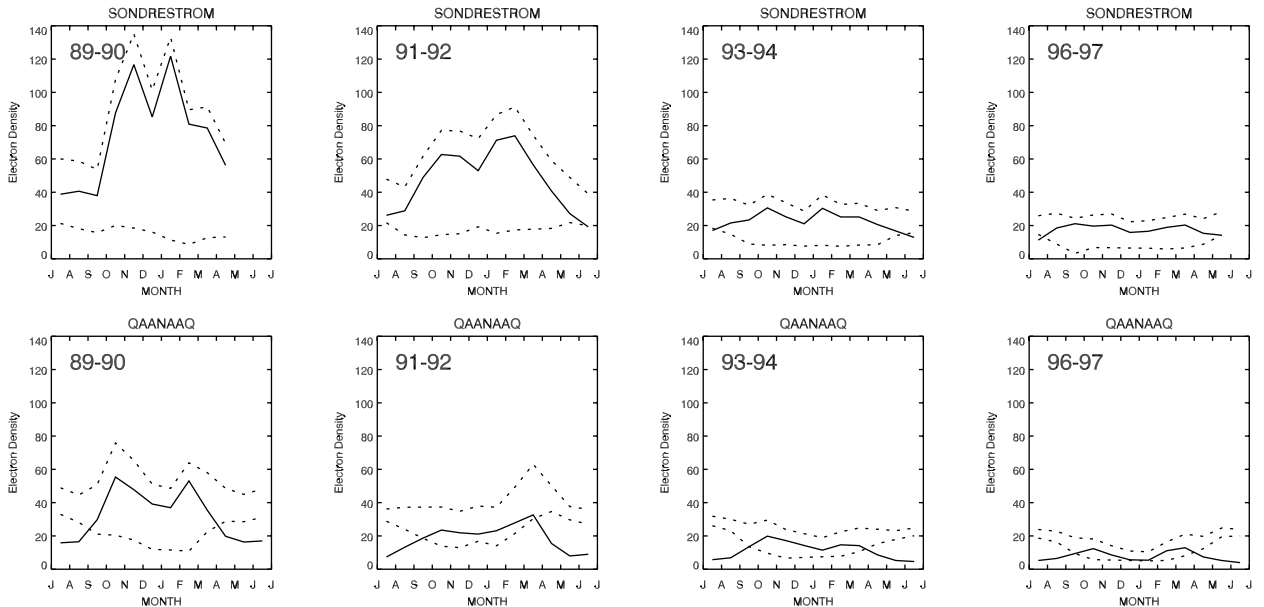


**Figure 9.** Seasonal variation in electron density at  $\pm \delta$  levels at Sondrestromfjord and Qaanaaq for the years 1989–1990, 1991–1992, 1993–1994, and 1996–1997, with averaged SSN reducing from 150 to 10. The  $y$  scale for electron density extends from 0 to  $200 \times 10^4 \text{ cm}^{-3}$ .

at a given time over all the year. The results are presented in Figure 7. At Sondrestromfjord a strong and wide regular peak is seen between 1200 UT and 2000 UT at all patch strengths irrespective of the level of sunspot activity. However, at a given patch strength the occurrence level drops with decreasing solar activity. For example, at the 5-MHz level the peak occurrence of 60% during high sunspot numbers of 120–150 seen in Figures 7a and 7b drops to less than 10% at the lowest sunspot number in Figure 7d. This effect is due to change in the strength of the tongue of ionization, which will be discussed a little later. At Qaanaaq the polar cap patch activity peaks around 1800 UT and is at a minimum around 1200 UT. Thus the peak activity occurs a few hours after magnetic noon. The peak activity of 60% during times of high sunspot numbers (120–150) seen in Figures 7e and 7f for patch strength  $\geq 4$  MHz drops to 20% at the low sunspot number of 10 in Figure 7h. *Basu et al.* [1995] noted that at Thule (100 km south of Qaanaaq), scintillation activity (associated with polar cap patches) is low between 0800 and 1200 UT and high between 2000 and 2400 UT. From satellite observations, *Coley and Heelis* [1995] note that the patches occur more often between 1200 and 2000 UT peaking around 1800 UT. *Coley and Heelis* [1998b] rightly state that the patches are a winter phenomenon indicating that the polar cap must be predominantly in darkness. The mechanism [*Anderson et al.*, 1988; *Decker et al.*, 1994; *Valladares et*

*al.*, 1996; *Coley and Heelis*, 1998b; *Basu and Valladares*, 1999] operates more effectively when the convection pattern is closer to the day terminator and has the longest residence time in sunlight for the formation of the tongue of ionization. These conditions occur near 1800 UT in winter in the Northern Hemisphere. Therefore polar cap patch occurrence peaks around 1800 UT.

[14] Figure 8 shows the diurnal variation of electron density at Sondrestromfjord and Qaanaaq for the summer (July) and winter (December) months for four levels of sunspot activity. Each graph presents three levels: median and  $\pm \sigma$  of the variation of electron density. At Sondrestromfjord in the summer months the electron density at all three levels is reasonably flat at all levels of sunspot activity. The difference between the top and the bottom level would be a measure of electron density available for the producing the patches. Therefore in summer months the plasma source resulting in the patches is weak and reduces in strength with declining sunspot activity. In the figure the second row presents the electron density at Qaanaaq. At Qaanaaq, similar to the activity at Sondrestromfjord, in summer, polar cap patches would be weak and show a further decline in strength with declining solar activity.

[15] In Figure 8 the third row presents results for Sondrestromfjord. In winter months the electron density shows a regular increase between 1200 and 1800 UT with a peak around 1500 UT. The strength of the peak (Decem-



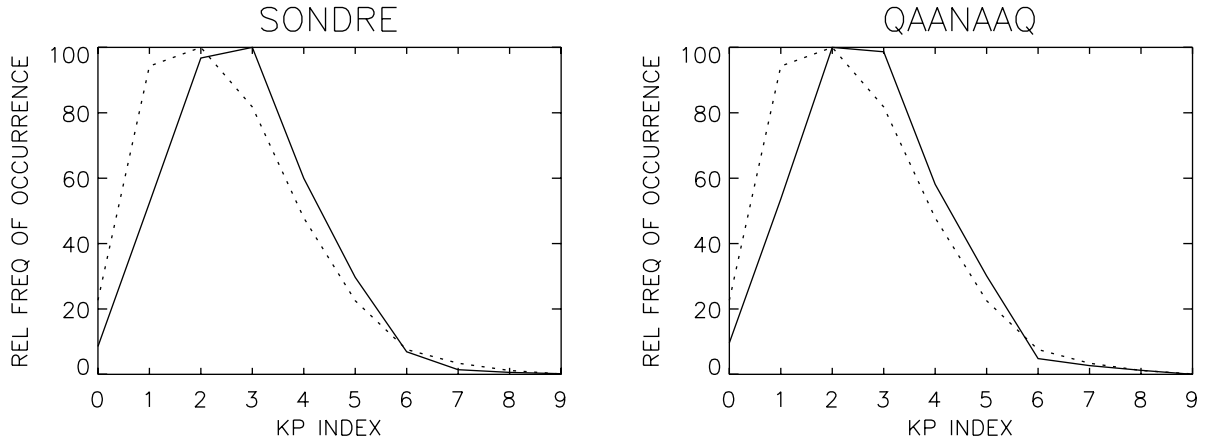


**Figure 10.** Distribution of the planetary geomagnetic  $Kp$  for the polar cap patch activity and in the  $Kp$  index database for the stations Sondrestromfjord and Qaanaaq.

ber 1989) is strongest at highest sunspot number and reduces in strength with declining sunspot number. *Weber et al.* [1984] and *Pedersen et al.* [1998, 2000] showed that this peak electron density, called the tongue of ionization (TOI), is a source of the density seen within the polar cap patches and that these solar-produced patches move in the antisunward direction. The difference between the top and bottom curves at Qaanaaq shows behavior similar to that at Sondrestromfjord. At Qaanaaq the peak occurs around 1800 UT whereas at Sondrestromfjord the peak occurs around 1500 UT. This is consistent with the assumption that the patches are formed on the dayside at the high-latitude cusp region of Sondrestromfjord and drift to the darker polar latitudes of Qaanaaq. A reduction in the occurrence of polar cap patches with declining sunspot activity seen in Figures 1–3 is due to the decline in the strength of the source (TOI) with sunspot activity seen in Sondrestromfjord data in the third row of Figure 8.

[16] The seasonal variation of electron content available for the formation of a tongue of ionization at Sondrestromfjord, which may be seen in form of polar cap patches at Qaanaaq, is determined in the following manner. Levels of  $\pm \delta$  distributions of monthly diurnal variation such as those shown in Figure 8 are used. From these two levels the maximum and minimum determined for each month are shown in Figure 9 for stations Sondrestromfjord and Qaanaaq. In each graph a pair of dashed curves show the monthly maximum and minimum at the  $\pm \delta$  levels of diurnal variation, and the solid curve shows the difference between the dashed curves. The solid curve shows the electron density that contributes to TOI at Sondrestromfjord and to polar cap patches at Qaanaaq. A feature common to all these graphs is the

bimodal distribution of electron density with peaks around the months of October–November and February–March. The averaged sunspot number (SSN) decreased from 150 in 1989–1990 to 10 in 1996–1997. At both the stations the strength of these peaks reduced by a factor of 5 during this period. This behavior explains the overall variations in polar cap patches shown in Figures 1–3 and their seasonal variations shown in Figure 4. The stronger patches observed occur in the months of October–November and February–March, which are the periods of occurrence of high electron density seen in Figure 9.

[17] At Sondrestromfjord for high sunspot numbers of 125–150 in 1989–1992, the time width of the polar cap patches was found to increase from 60 to 90 min with an increase in patch strength from 3 MHz to 9 MHz. On the other hand, at Qaanaaq for the same period, the time width was found to decrease from 60 to 45 min. The difference in time widths and their difference in behavior at two stations can be explained by noting that the patches originate at the latitude of Sondrestrom and, while drifting to the polar latitude of Qaanaaq, the patches dissipate because of ionospheric recombination. At both stations, for medium (SSN = 40) and low (SSN = 10) sunspot activity, patch strengths were weaker, and the time width was about 45 min. The peak to peak separation was about 110 min at Sondrestromfjord and 90 min at Qaanaaq for all these years. A good number of observations (*Buchau et al.* [1983], *Weber et al.* [1984, 1986], *Rodger et al.* [1994b], *Fukui et al.* [1994], *Obara et al.* [1996], *Kivanc and Heelis* [1997], and others) have shown that the velocity of patches is in the range of 400–800 m s<sup>-1</sup>. Using an average velocity of 600 m s<sup>-1</sup>, the

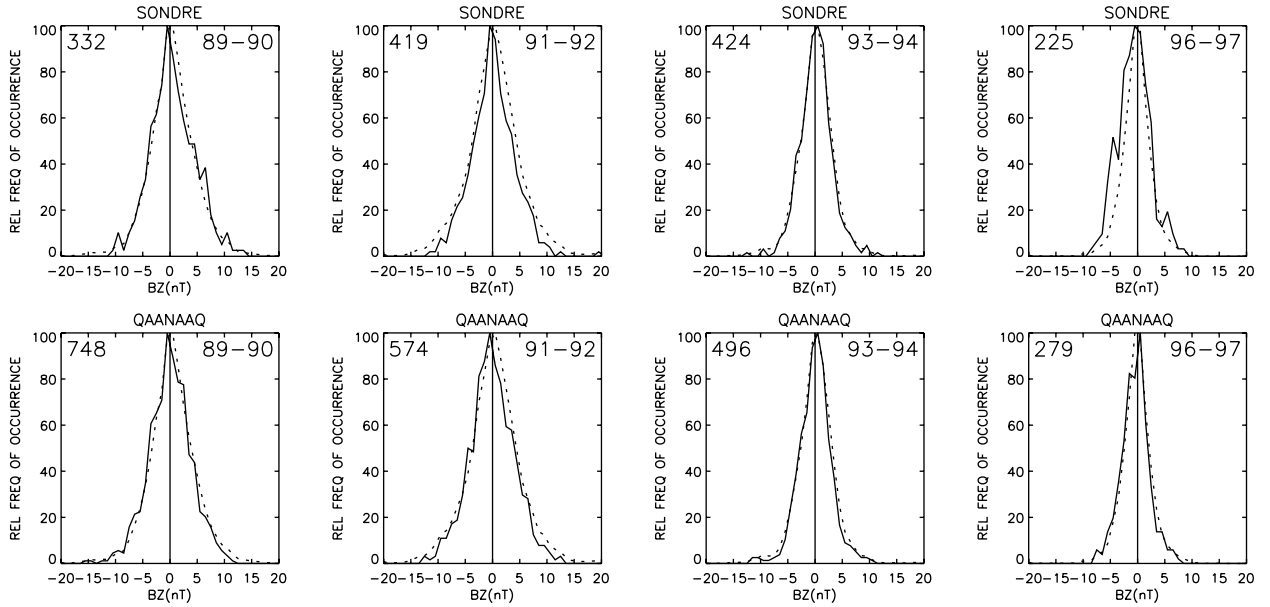


**Figure 11a.** Distribution of  $b_z$  component of interplanetary magnetic field (IMF) for polar cap patch activity at Sondrestromfjord and Qaanaaq (solid curves, average of 30, 20, and 10 min lead; dashed curves, distribution in the IMF database).

patch size is 2100 km at Sondrestromfjord and reduces to 1600 km at Qaanaaq; thus our estimations are slightly on the high side. *Weber et al.* [1985] determined the patch size as 1000 km. Our results are reasonably consistent with those of *Weber et al.* [1985], *Buchau et al.* [1983], *Coley and Heelis* [1995], and others. The patch size is found to decrease with decreasing sunspot activity.

[18] A distance of 1230 km separates the stations Sondrestromfjord and Qaanaaq. It is not possible to track the patches from one station (Sondrestromfjord) directly to the other using two digisondes. Assuming that the patches originating at Sondrestromfjord move poleward toward Qaanaaq and the dissipation period for patches is a few hours because of ionospheric recombination, only about 30% of patches at Qaanaaq occur within 2 hours of patches at Sondrestromfjord, with patch strength ratio  $\leq 1$  with respect to that at Sondrestromfjord. The remaining 70% have either a patch strength ratio  $\geq 1$  and/or time differences of more than 2 hours compared to those at Sondrestromfjord and thus are not related to the patch activity at Sondrestromfjord.

### 3.3. Dependence of Polar Cap Patch Activity on Magnetic Activity

[19] For studying the effect of magnetic activity on the behavior of polar cap patches, data of planetary magnetic activity index  $Kp$  and of interplanetary mag-

netic field (IMF) are used. A few case studies have indicated that polar cap patches occur on magnetically disturbed days with daily  $\Sigma Kp \geq 25$  [*Buchau et al.*, 1983]. The large data set of 4 years of the present study shows that the probability of patch occurrence is independent of the whole day's level of magnetic activity. From all the data of 4 years covering different levels of solar activity, and from  $f_oF_2$  observations for the duration of which the polar cap patches were seen, the population distributions of 3-hour  $Kp$  indices were determined. The normalized distributions are shown in Figure 10. For both stations there is a definite tendency for the patches to occur more frequently with increasing level of magnetic activity. This is consistent with case studies (*Buchau et al.* [1983], *Weber et al.* [1984], and others). A study of strong patches ( $\geq 7$  MHz for 1989–1992,  $\geq 6$  MHz for 1993–1994, and  $\geq 5$  MHz for 1996–1997, respectively) did not show any stronger dependence on  $Kp$  than that shown in Figure 10. These strong peaks are seen in the winter season when electron density is high (see Figure 9). It is observed that the patch occurrence is primarily diurnally dependent and its  $Kp$  dependence is secondary.

[20] To use the interplanetary magnetic field (IMF) data, 8-s IMF data were averaged over 1-min intervals. The components ( $b_x$ ,  $b_y$ ,  $b_z$ ) of the IMF data were divided into time sequences of positive and negative polarity. As

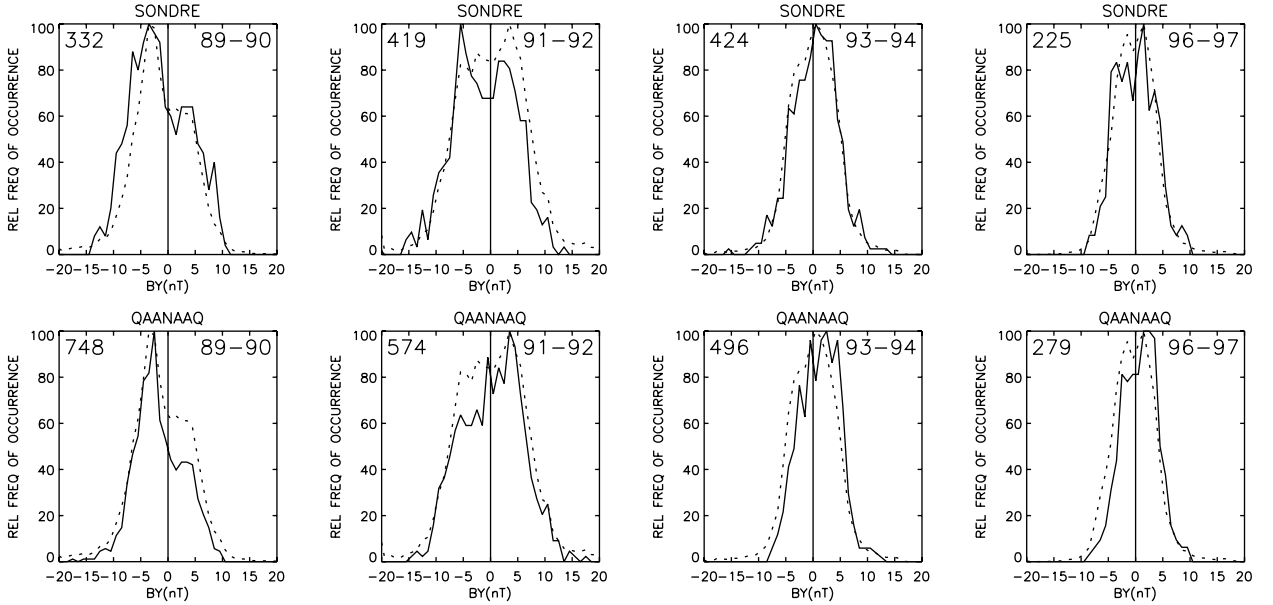


**Figure 11b.** Distribution of  $b_y$  component of interplanetary magnetic field (IMF) for polar cap patch activity at Sondrestromfjord and Qaanaaq.

the IMF data are not usable when the satellite is inside the magnetopause, reliable IMF data are available for about 28% of the patches seen in the  $f_oF_2$  data. A distribution of each component in 1-nT intervals was determined from the IMF database. Lead time intervals of 30, 20, and 10 min for the IMF with respect to the start time of patches were used for studying the patch dependence on the IMF. As the IMF distribution for the patches for these three (time interval) groups was very similar, all these groups were averaged. The results are presented in Figures 11a–11c for the IMF components  $b_z$ ,  $b_y$ , and  $b_x$ , respectively. In each figure each graph has a station heading. The observation period is marked in the right-hand top corner of each graph, and the number of patches with the IMF data are listed in the left-hand top corner. The solid curve shows a normalized IMF distribution for patches, and the dashed curve shows a normalized distribution of the IMF database. In Figures 11a–11c, one of the striking common features for each individual graph is a very close similarity in the shapes of all the data for the IMF component (dashed curve) and that for the patches (solid curve). In Figure 11a both the distributions for  $b_z$  peak at  $-1$  nT for the high-sunspot years 1989–1982, whereas these peak at  $+1$  nT in 1993–1994 and at  $+2$  nT in 1996–1997. In Figure 11b the  $b_y$  component for the IMF database peaks at  $-3$  nT,  $-6$  nT,  $+1$  nT, and  $+2$  nT for the respective years. At

Sondrestromfjord for the patches the respective values are  $-4$  nT,  $-6$  nT,  $+1$  nT, and  $+2$  nT. For the sake of completeness, Figure 11c shows the distribution for the  $b_x$  component. The IMF database shows a bimodal distribution, and the stronger peaks are at  $+4$  nT,  $-6$  nT,  $-3$  nT, and  $-3$  nT, respectively. The feature common to all these figures is that the IMF for the patch occurrence very closely follows the same distribution as that of the IMF database. A study of strong patches ( $\geq 7$  MHz for 1989–1992,  $\geq 6$  MHz for 1993–1994, and  $\geq 5$  MHz for 1996–1997, respectively) did not show any distinct dependence on  $b_x$ ,  $b_y$ , and  $b_z$  components of the IMF.

[21] In an 18-month period from August 1981 to February 1983, *Coley and Heelis* [1995] observed 281 patches at invariant latitude greater than  $70^\circ$ , with an enhancement factor greater than 2. They found 143 cases with  $b_z$  negative and 150 cases with  $b_z$  positive. *McEwen and Harris* [1996] found 143 cases with  $b_z$  negative and 39 cases with  $b_z$  positive. *Rodger and Graham* [1996] looked at HF radar data from Halley, Antarctica, for 2 years (1989–1990) and did not find any correlation with IMF. Component  $b_z$  was  $-3$  nT for the patches, which is also the average for the data period. Our results are in good agreement with these results. Thus, for a small percent of cases with favorable IMF conditions, certain mechanisms would be able to explain the generation of polar cap patches, but a large number of remaining cases

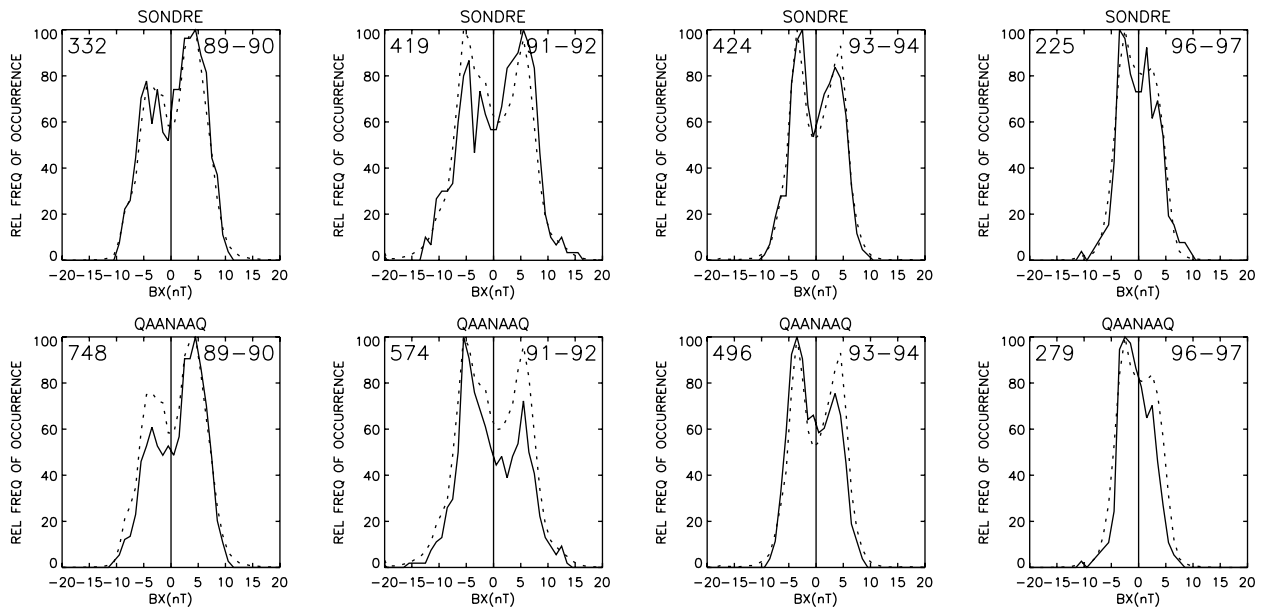


**Figure 11c.** Distribution of  $b_x$  component of interplanetary magnetic field (IMF) for polar cap patch activity at Sondrestromfjord and Qaanaaq.

indicate a need to look at additional mechanisms [see *Tsunoda*, 1988] for the generation of patches.

[22] In general about 25% of the patches are associated with a change in the sign of a given component ( $b_x$ ,  $b_y$ ,  $b_z$ ) of the IMF, but the number of cases divided equally for either sign of polarity. Thus only about 13% of the data are associated with, for example, a change from  $b_z$  positive (northward) to  $b_z$  negative (southward), satisfying a definition of the polar cap patch.

[23] *Valladares et al.* [1998a] have shown that sometimes polar cap arcs can be embedded in the polar cap patches. At present the general understanding (for example, see the review by *Basu and Valladares* [1999]) is that the tongue of ionization formed at the dayside cusp region is a source for the polar cap patches. A change in the polarity from  $b_z$  positive (northward) to  $b_z$  negative (southward) results in the generation of polar cap patches, and the patches drift in the antisunward direction. Once the patches are formed and start drifting, their duration is controlled only by dissipation (and not by the sign of the  $b_z$  polarity) and by the loss due to recombination. On the other hand, the polar cap arcs are associated with the switch of  $b_z$  polarity from positive to negative, the arcs drift from dusk to dawn, and they disappear when the  $b_z$  polarity reverses from negative to positive. At present, from the DISS measurements alone it is not possible to strictly categorize the observed patches as polar cap patches that are drifting in the

antisunward direction. The added capability of drift measurements of the DISS system may help to resolve this problem in future observations.

### 3.4. Mechanisms for Generation of Polar Cap Patches

[24] Let us now consider various mechanisms for the generation of polar cap patch activity. *Tsunoda* [1988] and *Crowley* [1996] have reviewed several mechanisms for formation of the polar cap patches. At present the general understanding is that polar cap patches are not associated with particle precipitation but are solar produced at subauroral latitudes and, under the influence of high-latitude convection pattern, are transported from the cusp region to the polar region moving in the antisunward direction [*Weber et al.*, 1984]. The patches usually start occurring after the IMF  $b_z$  polarity changes from positive (northward) to negative (southward) and also shows  $b_y$  dependence [*Fukui et al.*, 1994]. Our observations show that only about 13% of the cases satisfy this condition of occurring (between 10 and 30 min) after the IMF  $b_z$  polarity changes from positive (northward) to negative (southward).

[25] For the chopping of the tongue of ionization (TOI) into the formation of discrete patches several mechanisms have been suggested by different workers. *Anderson et al.* [1988] suggested a sudden expansion of the

polar cap region to lower latitudes. This would add higher-density plasma to the polar cap region. *Rodger et al.* [1994a] argue that such expansion events do not occur that often to explain the large number of patches seen in the polar cap. One of the most promising mechanisms for chopping the TOI is a frequent change in the convection pattern in response to changes in the  $b_y$  component of the IMF. The IMF is so variable that there may be ample opportunities to generate patches to support the observed frequency of occurrence. This mechanism has been studied in detail by *Decker et al.* [1994], *Sojka et al.* [1994], *Bowline et al.* [1996], and *Steele and Cogger* [1996].

[26] *Sojka et al.* [1994] simulated the polar cap patch behavior for high solar activity with solar flux equal to  $210 \text{ W m}^{-2}$  and  $Kp = 3.5$ . They used the Utah State University time-dependent ionospheric model (TDIM). For chopping the TOI, while holding  $b_z$  negative, they flip-flopped the  $b_y$  component between two extreme values:  $b_y$  positive “A” and  $b_y$  negative “DE” plasma convection patterns described by *Heppner and Maynard* [1987]. The patch thus generated would continue to drift for several hours as the decay time because ionospheric recombination is of the order of a few hours. This persistence of a patch beyond its time of generation explains a lack of correlation with IMF seen in observations in this study. This mechanism satisfactorily explains the diurnal and seasonal variations observed in the present study. *Coley and Heelis* [1998a] separated patches according to  $b_z$  polarity. They suggest that for  $b_z$  negative, patches form near the cusp and convect across the polar cap. They postulate that for  $b_z$  positive the mechanism would be local differences in the convective flow for adjacent regions near the dayside terminator, resulting in more structured patches.

[27] *Rodger et al.* [1994a] and *Valladares et al.* [1994] suggest the flux transfer event and associated convection jets called flow channel events (FCE) as an additional mechanism for the generation of polar cap patches. They postulate that high-speed flow in an FCE convection vortex generates Joule heating and thus increases the plasma temperature. This increases the ion recombination rate, with a consequent reduction of the  $F$  region plasma density. Thus the TOI is intermittently reduced and chopped into discrete patches. This mechanism needs to be further investigated. *Valladares et al.* [1998b] rightly state that the  $b_z$  switching mechanism does not exclude the validity of other patch formation mechanisms; it merely suggests that a  $b_z$  northward TOI can end up as a polar cap patch if a timely reversal of  $b_z$  from

positive to negative occurs. *Rodger and Graham* [1996] feel that flux transfer events should be incorporated in the *Sojka et al.* [1994] model.

### 3.5. Effects on Communication, Surveillance, and Navigation Systems

[28] Now let us briefly and qualitatively consider a range of disruption of these systems by the occurrence of polar cap patch activity. Using radio scintillation and  $f_oF_2$  data from Sondrestromfjord and Qaanaaq, *Dandekar and Bullett* [1999] found a linear relation between patch strength in  $f_oF_2$  (megahertz) and scintillation index measured at 250 MHz in decibels (dB). They found that (approximately) each megahertz increase in polar cap patch strength corresponds to an increase the scintillation index of about 2.5–3 dB. From Figure 3, for a minimum patch activity of 30% the scintillation index increases from 10 dB (4 MHz) to 25 dB (8 MHz). Our present results show that for weak patches (3 MHz) the frequency of patch occurrence (Figure 4) increases by a factor of 3 from 15% at low sunspot activity to 50% at high sunspot activity. At a patch strength of  $\geq 5$  MHz the occurrence is hardly 5% for sunspot activity  $SSN \leq 40$ . It increases to about 20%, a factor of 4, at high sunspot activity. In addition, the patch strength rises as high as 9–10 MHz; thus the patch strength increases ( $\propto f_oF_2^2$ ) by a factor of 3. Also there is a systematic seasonal increase in patch activity in winter months. For example, in Figure 6 for Sondrestromfjord the patch activity shows a seasonal change from 20% nonwinter to 70% in winter, an increase by a factor of 3. Thus systems operating (for communication, surveillance, and navigation) in polar regions would experience tremendous disruptions due to a wide range of polar cap activity in terms of duration, season, and patch strength associated with solar cycle activity.

## 4. Conclusions

[29] This study presents a long-term behavior of polar patches covering the declining solar cycle activity from  $SSN = 150$  in 1989–1990 to  $SSN = 10$  in 1996–1997. Because the polar cap patches may severely degrade the operation of space surveillance and navigation systems operating at high latitudes, it is useful to determine the range of change the systems will experience due to polar cap patch activity. The results presented show a systematic reduction in the polar cap patch activity (with declining sunspot activity) with respect to the number of patches per day, patch strength, duration, and season. At patch strength  $\geq 3$  MHz the number of patches is

reduced from six per day to three per day and from eight per day to four per day (see Figure 2) at Sondrestromfjord and Qaanaaq, respectively, with declining sunspot number (SSN). For strong patches ( $\geq 7$  MHz) with a given level of solar activity this number reduces by 50%. At low solar activity, strong patches ( $\geq 7$  MHz) are rare at both the stations. At high solar activity the frequency of occurrence is 85% for patch strength  $\geq 3$  MHz (see Figure 3) and drops to 45% for strong patches ( $\geq 7$  MHz), whereas it drops to less than 5% at low solar activity. Similarly, the frequency of occurrence based on the period of duration (see Figure 4) reduces from 50% to 10% for patch strength  $\geq 3$  MHz and from 15% to less than 2% with declining solar activity. Thus the polar cap patch activity changes by an order of magnitude over a solar cycle. The patch occurrence peaks around magnetic noon. Using case studies, several workers have suggested dependence of polar cap patch activity on magnetic activity. A look at the large number of cases covered here shows that diurnal, seasonal, and solar cycle dependence of polar cap activity is predominant and dependence on magnetic activity index  $Kp$  is secondary. The IMF population distribution with respect to the time of occurrence of patches does not show any distinct dependence of patch activity on the  $b_x$ ,  $b_y$ , and  $b_z$  components of the IMF. The numerical simulations conducted by Sojka *et al.* [1994] for high solar activity adequately explain these observations. Various other mechanisms suggested for the generation of polar cap patches need further investigation.

[30] **Acknowledgments.** The author thanks C. E. Valladares and S. Basu for their valuable comments on the paper.

## References

- Anderson, D. N., J. Buchau, and R. A. Heelis, Origin of density enhancements in the winter polar cap ionosphere, *Radio Sci.*, **23**, 513–519, 1988.
- Basu, S., and C. Valladares, Global aspects of plasma structures, *J. Atmos. Sol. Terr. Phys.*, **61**, 127–139, 1999.
- Basu, S., S. Basu, J. J. Sojka, R. W. Schunk, and E. MacKenzie, Macroscale modeling and mesoscale observations of plasma density structures in the polar cap, *Geophys. Res. Lett.*, **22**, 881–884, 1995.
- Behnke, R. A., T. F. Tascione, E. Hildner, W. Cliffswallow, R. M. Robinson, N. E. Cobb, A. W. Green, S. Basu, O. de la Beaujardiere, and R. L. Carovillano, The National Space Weather Program: Strategic plan, *Rep. FCM-P30-1995*, Off. of the Fed. Coord. for Meteorol. Serv. and Supporting Res., Silver Spring, Md., 1995.
- Bowline, M. D., J. J. Sojka, and R. W. Schunk, Relationship of theoretical patch climatology to polar cap patch observations, *Radio Sci.*, **31**, 635–644, 1996.
- Buchau, J., and B. W. Reinisch, Electron density structures in the polar  $F$  region, *Adv. Space Res.*, **11**(10), 29–37, 1991.
- Buchau, J., B. W. Reinisch, E. J. Weber, and J. G. Moore, Structure and dynamics of the winter polar cap  $F$  region, *Radio Sci.*, **18**, 995–1010, 1983.
- Coley, W. R., and R. A. Heelis, Adaptive identification and characterization of polar ionization patches, *J. Geophys. Res.*, **100**, 23,819–23,827, 1995.
- Coley, W. R., and R. A. Heelis, Structure and occurrence of polar ionization patches, *J. Geophys. Res.*, **103**, 2201–2208, 1998a.
- Coley, W. R., and R. A. Heelis, Seasonal and universal time distribution of patches in the northern and southern polar caps, *J. Geophys. Res.*, **103**, 29,229–29,237, 1998b.
- Crowley, G., Critical review of ionospheric patches and blobs, *The Reviews of Radio Science 1992–1996*, edited by W. R. Stone, pp. 619–648, Oxford Univ. Press, New York, 1996.
- Dandekar, B. S., and T. W. Bullett, Morphology of polar cap patch activity, *Radio Sci.*, **34**, 1187–1205, 1999.
- Decker, D. T., C. E. Valladares, R. Sheehan, S. Basu, D. N. Anderson, and R. A. Heelis, Modeling daytime  $F$  layer patches over Sondrestrom, *Radio Sci.*, **29**, 249–268, 1994.
- Fukui, K., J. Buchau, and C. E. Valladares, Convection of polar cap patches observed at Qaanaaq, Greenland, during the winter of 1989–1990, *Radio Sci.*, **29**, 231–248, 1994.
- Heppner, J. P., and N. C. Maynard, Empirical high latitude electric field models, *J. Geophys. Res.*, **92**, 4467–4489, 1987.
- Kivanc, O., and R. A. Heelis, Structures in ionospheric number density and velocity associated with polar cap ionization patches, *J. Geophys. Res.*, **102**, 307–318, 1997.
- McEwen, D. J., and D. P. Harris, Occurrence patterns of  $F$  layer patches over north magnetic pole, *Radio Sci.*, **31**, 619–628, 1996.
- Obara, T., T. Mukai, A. Hayakawa, A. Matsukova, K. Tsuruda, A. Nishida, K. Fukui, J. V. Rodriguez, and C. E. Valladares, Simultaneous satellite and all-sky imager observations of polar cap phenomena, *J. Geomagn. Geoelectr.*, **48**, 935–946, 1996.
- Pedersen, T. R., B. G. Fejer, R. A. Doe, and E. J. Weber, Incoherent scatter radar observations of horizontal  $F$  region plasma structure over Sondrestrom, Greenland, during polar cap patch events, *Radio Sci.*, **33**, 1847–1866, 1998.
- Pedersen, T. R., B. G. Fejer, R. A. Doe, and E. J. Weber, An incoherent scatter radar technique for determining two-dimensional horizontal ionization structure in polar cap  $F$  region patches, *J. Geophys. Res.*, **105**, 10,637–10,655, 2000.
- Reinisch, B. W., R. R. Gamache, J. S. Tang, and D. F. Kitrosser, Automatic real time ionogram scaler with true height analysis: ARTIST, *AFGL-TR-83-0209*, Air Force Geophys. Lab., Bedford, Mass., 1983.

- Rodger, A. S., and A. C. Graham, Diurnal and seasonal occurrence of polar cap patches, *Ann. Geophys.*, *14*, 533–537, 1996.
- Rodger, A. S., S. M. Pinnock, and J. R. Dudeney, Comment on “Production of polar cap electron density patches by transient magnetopause reconnection” by M. Lockwood and H. C. Carlson Jr., *Geophys. Res. Lett.*, *21*, 2335–2336, 1994a.
- Rodger, A. S., S. M. Pinnock, J. R. Dudeney, K. B. Baker, and R. A. Greenwald, A new mechanism for polar cap formation, *J. Geophys. Res.*, *99*, 6425–6436, 1994b.
- Sojka, J. J., M. D. Bowline, and R. W. Schunk, Patches in the polar ionosphere: UT and seasonal dependence, *J. Geophys. Res.*, *99*, 14,959–14,970, 1994.
- Steele, D. P., and L. L. Cogger, Polar patches and the “tongue of ionization”, *Radio Sci.*, *31*, 667–677, 1996.
- Tsunoda, R. T., High-latitude *F* region irregularities: A review and synthesis, *Rev. Geophys.*, *26*(4), 719–760, 1988.
- Valladares, C. E., S. Basu, J. Buchau, and E. Friis-Christensen, Experimental evidence for the formation and entry of patches into the polar cap, *Radio Sci.*, *29*, 167–194, 1994.
- Valladares, C. E., D. T. Decker, R. Sheehan, and D. N. Anderson, Modeling the formation of polar cap patches using large plasma flows, *Radio Sci.*, *31*, 573–594, 1996.
- Valladares, C. E., K. Fukui, R. Sheehan, H. C. Carlson Jr., and T. Bullett, Simultaneous observations of polar cap patches and sun-aligned arcs during transition of the IMF, *Radio Sci.*, *33*, 1829–1845, 1998a.
- Valladares, C. E., D. T. Decker, R. Sheehan, D. N. Anderson, T. Bullett, and B. W. Reinisch, Formation of polar cap patches associated with north-to-south transitions of the interplanetary magnetic field, *J. Geophys. Res.*, *103*, 14,657–14,670, 1998b.
- Weber, E. J., J. Buchau, J. G. Moore, J. R. Sharber, R. C. Livingstone, J. Winningham, and B. W. Reinisch, *F* layer ionization patches in the polar cap, *J. Geophys. Res.*, *89*, 1683–1694, 1984.
- Weber, E. J., R. T. Tsunoda, J. Buchau, R. E. Sheehan, D. J. Strickland, W. Whiting, and J. G. Moore, Coordinated measurements of auroral zone plasma enhancements, *J. Geophys. Res.*, *90*, 6497–6513, 1985.
- Weber, E. J., J. Klobuchar, J. Buchau, H. C. Carlson, R. C. Livingston, O. de la Beaujardiere, M. McCready, J. G. Moore, and G. J. Bishop, Polar cap *F* layer patches: Structure and dynamics, *J. Geophys. Res.*, *91*, 12,121–12,129, 1986.
- 
- B. Dandekar, Air Force Research Laboratory, Space Vehicles Directorate, Hanscom AFB, MA 01731-3010, USA. (balkrishna.dandekar@hanscom.af.mil)